IEEE Access
Multidisciplinary | Rapid Review | Open Access Journal

Received April 23, 2022, accepted May 8, 2022, date of publication May 13, 2022, date of current version May 19, 2022.

Digital Object Identifier 10.1109/ACCESS.2022.3174871

Robust Adaptive Observer-Based Predictive Control for a Non-Linear Delayed Bilateral Teleoperation System

LINPING CHAN[1], YANG LIU[1], QINGQING HUANG[1,2], (Member, IEEE), AND PING WANG[1,2]
[1]Key Laboratory of Industrial Internet of Things and Networked Control, Chongqing University of Posts and Telecommunications, Chongqing 400065, China
[2]Institute of Industrial Internet, Chongqing University of Posts and Telecommunications, Chongqing 401120, China

Corresponding author: Qingqing Huang (huangqq@cqupt.edu.cn)

This work was supported in part by the National Key Research and Development Program of China under Grant 2018YFB1700200, and in part by the Venture and Innovation Support Program for Chongqing Overseas Returnees under Grant cx2021026.

ABSTRACT In this paper, a new robust adaptive nonlinear teleoperation system using an improved extended active observer (IEAOB), adaptive Smith predictor (ASP) and sliding mode control is developed to address the time delay in the communication channels and the nonlinear robot model uncertainties. Firstly, an ASP based on Padé approximation and active observer is designed to compensate for the time delay effect. Specifically, the total network time delay is modelled by Padé approximation, and then an active observer is deployed to estimate the time delay. To ensure the time-varying delay effect is completely suppressed, a sliding mode control algorithm is further developed. The main added value of this teleoperation approach is that it requires neither specific mathematic delay-time model, nor strict assumptions on time delay from a practical point of view. Finally, the stability of the designed teleoperation system is theoretically studied and the system effectiveness is demonstrated by applying it to a pair of Phantom Omni haptic devices connected via a communication channel with time-varying delays.

INDEX TERMS Delay compensation, disturbance suppression, adaptive Smith predictor, sliding mode control, improved extended active observer.

I. INTRODUCTION

Bilateral teleoperation systems, which render human operators the capability to achieve complex tasks over a long distance, have been a hot research topic in the control and robotics fields. Applications of teleoperation are numerous ranging from space operation, underwater exploration and mining, to handling toxic or nuclear materials, as well as, robotic-assisted surgical interventions [1]. The ultimate goal of teleoperation is to convey to the operator a sense of direct interaction with the environment. These systems offer great potential, but ensuring that the master and slave stations are connected in a coherent manner is a challenging task. Prominent among the most scientific challenges in bilateral teleoperation are the time delay in the communication channels and the largely unknown dynamics of master and slave robots, which significantly deteriorate system performance and even jeopardize system stability.

The associate editor coordinating the review of this manuscript and approving it for publication was Mohammad Alshabi.

Various control methods have been developed in the literature to handle the destabilization problem caused by time delay. At the early stage, the scattering theory was employed in teleoperation systems to develop controllers ensuring stability by making the communication channel a passive lossless transmission line [2]. The time-domain passivity control method [3] was proposed by implementing a time-domain passivity observer to identify the period where artificial damping was required to guarantee the passivity of the teleoperation system. The wave-variable-based control approach [4], [5] was designed to guarantee the system's stability by the enrolment of wave transform, where power signals were transformed into wave variables in the communication channels. However, these above passivity-based methods focus on system stability. When the time delay increases, it would cause wave reflection and position drift, and the practicality of the teleoperation system decreases due to the reduced transparency. Hence, many modifications [6]–[9] have been proposed for the wave-variable-based approaches to reinforce the system performance. There are other control methods

developed to address the time delay issue as well, such as Smith predictor-based control [10], [11], communication disturbance observer (CDOB) based control [12], [13], etc. The adaptive fuzzy Smith predictor-based controller [11] was employed to compensate for the time-varying delay effect to achieve the desired tracking performance, a virtual slave model was utilized at the master side to enhance the stability. The principle of the CDOB-based approach [13] is to lump all undesired effects of time delay into an entity called network disturbance, deploy the disturbance observer to estimate it and then feedback on the estimated network disturbance to compensate for the time delay effects. In addition, various nonlinearities and uncertainties, essentially existing in robot manipulators, have to be considered as more complex teleoperation tasks are increasing in recent years. Lots of control strategies have been proposed in the engineering community to cope with these problems, such as adaptive control [14]–[21], robust control [22]–[25], and neural network and fuzzy logic technique [11], [23]–[31], etc. The radial basis function neural network (RBFNN) based adaptive robust control method for time-varying delay teleoperation systems in [26] and [27] were proposed to identify teleoperation system dynamical parameters, and accordingly improved the system tracking performance.

Although many efforts have been made to fight against the time delay and nonlinear robot model uncertainties, most of the proposed methods in the literature require some conservative assumptions, such as a small upper bound on time delay, the upper limit on the time delay changing rate, and the accurate dynamic system model. Hence, it becomes important and necessary to develop new control methods with relaxed assumptions on communication time delays and system model for teleoperation systems.

In this paper, a robust adaptive observer-based predictive control scheme is developed to achieve the best performance in terms of transparency in a bilateral teleoperation system with eased assumptions about the time delay and robot dynamic model. By adopting IEAOB in our previous work [14], [15], [32], the human/environment force and robot dynamic model can be accurately estimated in the presence of various disturbances. On this basis, the work offers the following contributions:

The proposed robust adaptive observer-based predictive control scheme can compensate for large time-varying delays and suppress various disturbances from nonlinear dynamics, modelling uncertainties and measurement noises.

An adaptive Smith predictor (ASP) based on Padé approximation and active observer is developed to achieve great time delay effect cancellation performance. The Padé approximation is utilized to model the round-trip time-varying delay, and there is no assumption about the upper limit of time delay changing rate.

In order to fully suppress the undesired effect of the time delay, the sliding mode control is further designed on the master side.

The remainder of this paper is organized as follows. The nonlinear dynamics of the master and slave devices and problem formulation are presented in Section II. In Section III, the proposed robust adaptive nonlinear teleoperation system is introduced, and its stability is theoretically studied. Section IV presents the application of the proposed teleoperation system to a nonlinear teleoperation system built by a pair of phantom haptic devices. Finally, conclusions are drawn in Section V.

II. PROBLEM FORMULATION

A nonlinear teleoperation system in the joint space can be formulated as

$$M_m(q_m,\theta_m)\ddot{q}_m + V_m(q_m,\dot{q}_m,\theta_m)\dot{q}_m + g_m(q_m,\theta_m) + T_{f_m} = T_m + T_h, \tag{1a}$$

$$M_s(q_s,\theta_s)\ddot{q}_s + V_s(q_s,\dot{q}_s,\theta_s)\dot{q}_s + g_s(q_s,\theta_s) + T_{f_s} = T_s - T_e, \tag{1b}$$

where $\ddot{q}_*, \dot{q}_*, q_*(* = m/s)$ are angular acceleration, angular velocity and angular position signals, $M_*(q_*, \theta_*)$ is the inertia matrix, $V_*(q_*, \dot{q}_*, \theta_*)$ is the vector of Coriolis and centripetal terms, $g_*(q_*, \theta_*)$ is the gravity torque,T_{f_*} are the friction torques, T_* are input torques of the controllers, θ_* represent inertial robotic parameters, and T_h, T_e correspond to the torques exerted by the human operator and environment, respectively. In this work, T_{f_*} is modeled as a simplified version of the LuGre model [33], by considering viscous and Coulomb friction,

$$T_{f_*} = v_{c_*} * sgn(\dot{q}_*) + v_{v_*} * \dot{q}_*, \tag{2}$$

where $v_{c_*} \in R^n$ is the coefficient vector of Coulomb friction, and $v_{v_*} \in R^n$ is the coefficient vector of viscous friction.

When one treats the external human/environment force acting on a manipulator as an unknown input and models it as a random walk process, and also considers that the master and slave robot dynamics are nonlinear with parameter variations, by defining the state vector $X_*(* = m/s)$ as $X_* = [\, q_* \;\; \dot{q}_* \;\; \theta_* \;\; v_{v_*} \;\; v_{c_*} \;\; T_{h/e} \,]'$, the teleoperation system model in (1) can be extended as follows:

$$\begin{aligned}\dot{X}_* &= f_*(X_*, T_*) + G_*\xi_{X_*} \\ &= \begin{bmatrix} \dot{q}_* \\ M_*^{-1}\left(-V_*\dot{q}_* - g_* - T_{f_*} + T_* \pm T_{h/e}\right) \\ 0 \\ 0 \\ 0 \\ 0 \end{bmatrix} \\ &\quad + G_* \begin{bmatrix} \xi_{q_*} \\ \xi_{\dot{q}_*} \\ \xi_{\theta_*} \\ \xi_{v_{v_*}} \\ \xi_{v_{c_*}} \\ \xi_{T_{h/e}} \end{bmatrix},\end{aligned} \tag{3a}$$

$$Y_* = H_* X_* + \eta_{X_*} = \begin{bmatrix} I & 0 & 0 & 0 & 0 & 0 \end{bmatrix} \begin{bmatrix} q_* \\ \dot{q}_* \\ \theta_* \\ v_{v_*} \\ v_{c_*} \\ T_{h/e} \end{bmatrix} + \eta_{X_*}, \tag{3b}$$

where Y_* is the output of the system, G_* is a unit matrix, and the state observation matrix $H_* = \begin{bmatrix} I & 0 & 0 & 0 & 0 & 0 \end{bmatrix}$, and ξ_{q_*}, $\xi_{\dot{q}_*}$ and η_{X_*} represent the process noises and measurement noises, respectively, $\xi_{T_{h/e}}$, $\xi_{v_{v_*}}$, $\xi_{v_{c_*}}$ and ξ_{θ_*} represent the rates at which the vectors of external torques, friction coefficients and robot parameters are estimated to vary.

Assume that the dynamic parameters of teleoperation manipulators are unknown but bounded, some important properties of the above nonlinear robot dynamic model are recalled as follows [30]:

Property 1: The inertia matrix $M_*(q_*)$ for a manipulator is symmetric positive-definite which verifies:

$$0 < \sigma_{min}(M_*(q_*)) I \leq M_*(q_*) \leq \sigma_{max}(M_*(q_*)) I \leq \infty, \tag{4}$$

where $I \in R^{n \times n}$ is the identity matrix. σ_{min} and σ_{max} denote the strictly positive minimum and maximum eigenvalue of M_* for all configurations $q_*(* = m/s)$.

Property 2: For a manipulator with revolute joints, there exists a positive Z bounding the Coriolis/centrifugal matrix as:

$$C_*(q_*(t), \dot{q}_*(t)) \dot{q}_*(t) \leq Z \|\dot{q}_*(t)\|_2^2. \tag{5}$$

In this paper, some assumptions are stated as:

Assumption 1: $t(t) = t_1(t) + t_2(t)$ represents the round-trip time delay, $t_1(t)$ is the forward communication channel-induced delay, $t_2(t)$ is the feedback communication channel-induced delay. It is assumed that the variable time-delays $t_*(t)$ have known upper bounds, i.e., $0 \leq t_*(t) \leq T_{max} < \infty, * = 1, 2$. It is reasonable to assume that the time-varying delay in the communication channel is bounded from a practical point of view. Infinite time delays imply that the connection between the master side and the slave side is broken.

Assumption 2: we assume that the operational torque and environmental torque are passive and satisfy [34]: there exist positive constants ρ such that

$$\left\| \begin{bmatrix} T_h \\ T_e \end{bmatrix} \right\|_2 \leq \rho, \tag{6}$$

where $\|X\|_2$ stands for the Euclidian 2-norm of a vector $X \in R^n$.

The control objective is to force the slave manipulator to greatly track the delayed master trajectory in the presence of time-varying delay and bounded parameter variation and external disturbances with an acceptable bounded tracking error.

III. DESIGN OF A ROBUST ADAPTIVE OBSERVER-BASED PREDICTIVE CONTROL SCHEME

A. THE PROPOSED TELEOPERATION ARCHITECTURE

Figure 1. shows the proposed control architecture for a nonlinear time-delayed bilateral teleoperation system. The master position signal $q_m(t)$ is transmitted to the slave in the forward communication channel $e^{-t_1 s}$, and the IEAOB is designed at the slave side to estimate the robot model parameters $(\hat{\theta}_s, \hat{v}_{c_s}, \hat{v}_{v_s})$ and environment torque $\hat{T}_e$. The PD controller T_s based on the estimated torque and robot model parameters $(\hat{\theta}_s, \hat{v}_{c_s}, \hat{v}_{v_s})$ is designed for the nonlinear slave manipulator to achieve great tracking performance under various disturbances and uncertainties. The estimated environment torque $\hat{T}_e$ is transmitted to the master via the feedback communication channel $e^{-t_2 s}$ to design the force controller at the master side. Based on the Padé approximation of the round-trip delay e^{-ts}, the active observer is employed on the master side to obtain the estimated time delay $\hat{t}(t)$, which is then used in the ASP design. As the ASP design relies on an accurate plant model, an IEAOB-based virtual slave model is built at the master side to generate the virtual estimated environment torque $\hat{T}_{ev}$. Considering that there is a small estimation error $e_t = t(t) - \hat{t}(t)$ for the time delay when designing the ASP, in order to further suppress the time delay effect, a sliding mode controller is developed. Meanwhile, the IEAOB is designed on the master side as well for the master robot to identify the dynamical model $\left(\hat{\theta}_m, \hat{v}_{c_m}, \hat{v}_{v_m}\right)$ and estimate the human operator torque $\hat{T}_h$, which is then used in the force controller design T_m under various disturbances and uncertainties. The master control design is simplified to let $\hat{T}_h$ track $\hat{T}_e$ as closely as possible. Therefore, good transparency performance can be obtained with the satisfied tracking performance for the slave robot and the actual feeling of estimated environmental torque provided for the human operator.

B. ADAPTIVE SMITH PREDICTOR BASED ON PADÉ APPROXIMATION, ACTIVE OBSERVER AND IEAOB

Figure 2. shows the schematic diagram of the proposed ASP for the teleoperation system. $t_1(t)$, $t_2(t)$ represent the time-varying delays at the forward and feedback communication channels, respectively. $t(t) = t_1(t) + t_2(t)$ is the round-trip time delay. $G_m(s)$ is the transfer function of the force controller and robot model at the master side, $G_s(s)$ is the transfer function of the position controller and robot model at the slave side. The transfer function of the ASP in the black dotted part in Figure 2.is written as follows:

$$G_{ASP}(s) = \frac{G_m(s)}{1 + (1 - e^{-\hat{t}s}) G_m(s) \hat{G}_s(s)}, \tag{7}$$

where $\hat{t}$ is the estimated round-trip time delay of $t(t)$.

The closed-loop transfer function for the teleoperation system involving the ASP is obtained as (8), shown at the bottom of the next page.

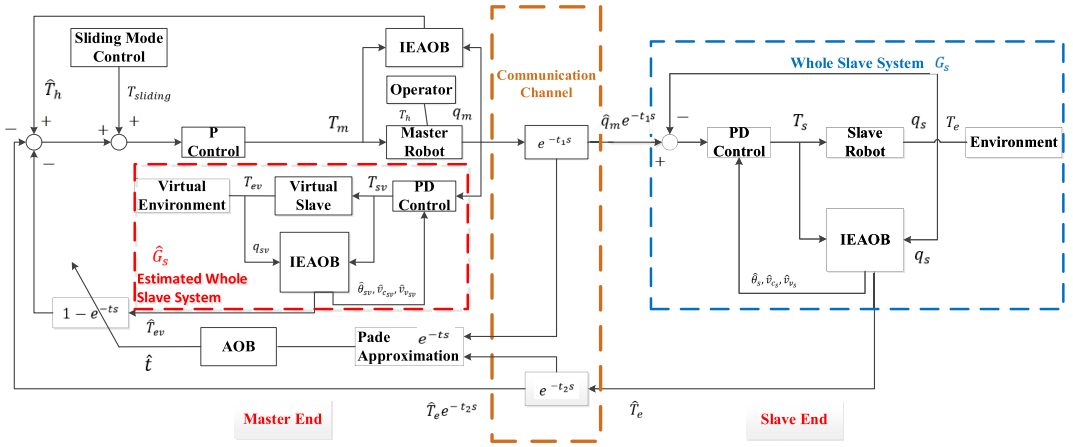

FIGURE 1. The proposed control architecture for bilateral teleoperation manipulators.

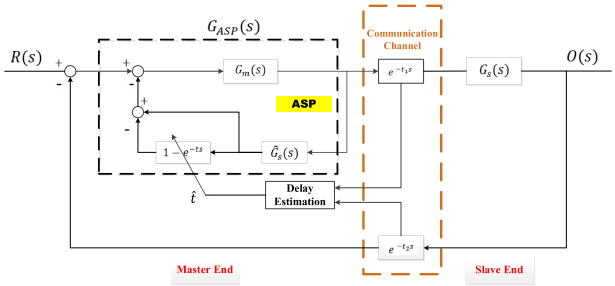

FIGURE 2. Block diagram of the proposed ASP.

It is easy to see that the effect of the time delay can be eliminated from the denominator and the system performance will not be affected by the time delay if

$$G_m(s)\,G_s(s)\,e^{-(t_1+t_2)s} - G_m(s)\,\hat{G}_s(s)\,e^{-\hat{t}s} = 0. \tag{9}$$

In order to satisfy (9), one needs to make

$$\hat{G}_s(s) = G_s(s), \tag{10a}$$

$$\hat{t} = t_1 + t_2, \tag{10b}$$

which implies that the success of the ASP depends on the accuracies of the estimations of both the slave model and the round-trip time delay.

In the next subsections, the design of the estimated virtual slave model with the IEAOB and the estimated round-trip time delay with Padé approximation will be presented.

1) ESTIMATION OF THE VIRTUAL SLAVE MODEL WITH THE IEAO

In order to provide the ASP with an accurate slave model, a virtual internal model (VIM) is built at the master side and the IEAOB is deployed to identify the nonlinear VIM and estimate the environment torque, as shown in the red dotted part of Figure. 1.

Specifically, let's consider the dynamic of the VIM as:

$$M_v(q_v,\theta_v)\,\ddot{q}_v + V_v(q_v,\dot{q}_v,\theta_v)\,\dot{q}_v + g_v(q_v,\theta_v) + T_{vf} = T_v - T_{ve}, \tag{11}$$

where $M_v(q_v,\theta_v)$ is the inertia matrix, $V_v(q_v,\dot{q}_v,\theta_v)$ is the vector of Coriolis and centrifugal terms, $g_v(q_v,\theta_v)$ is the gravity vector,$\ddot{q}_v \in R^n$, $\dot{q}_v \in R^n$, and $q_v \in R^n$ are the angular acceleration, angular velocity, and angular position vectors, respectively, T_v is the control torque vector, $\theta_v \in R^m$ represents a m-dimensional inertial robotic parameter vector, T_{vf} is the friction torque vector and defined in (2).

According to (3), the dynamical model in (11) can be re-written in state space form as:

$$\begin{aligned}\dot{X}_v &= f_v(X_v,T_v) + G_v\xi_{X_v} \\ &= \begin{bmatrix} \dot{q}_v \\ M_v^{-1}\left(-V_v\dot{q}_v - g_v - T_{vf} + T_v - T_{ve}\right) \\ 0 \\ 0 \\ 0 \\ 0 \end{bmatrix} \\ &\quad + G_* \begin{bmatrix} \xi_{q_v} \\ \xi_{\dot{q}_v} \\ \xi_{\theta_v} \\ \xi_{v_{vv}} \\ \xi_{v_{cv}} \\ \xi_{T_{ve}} \end{bmatrix},\end{aligned} \tag{12a}$$

$$\frac{O(s)}{R(s)} = \frac{G_m(s)G_s(s)e^{-t_1 s}}{1 + G_m(s)\,\hat{G}_s(s) - G_m(s)\,\hat{G}_s(s)\,e^{-\hat{t}s} + G_m(s)G_s(s)e^{-(t_1+t_2)s}} \tag{8}$$

$$Y_v = H_v X_v + \eta_{X_v} = \begin{bmatrix} I & 0\,0 & 0 & 0\,0 \end{bmatrix} \begin{bmatrix} q_v \\ \dot{q}_v \\ \theta_v \\ v_{v_v} \\ v_{c_v} \\ T_{ve} \end{bmatrix} + \eta_{X_v} \tag{12b}$$

where the state vector $X_v = [\, q_v \;\; \dot{q}_v \;\; \theta_v \;\; v_{v_v} \;\; v_{c_v} \;\; T_{ve} \,]'$.

Let's recall the design process of the IEAOB in [15], the IEAOB for the VIM is as follows:

$$\dot{\hat{X}}_v = f_v\left(\hat{X}_v, T_v\right) + P_v H_v^T R_v^{-1}\left(Y_v - H_v \hat{X}_v\right), \tag{13a}$$

where

$$\dot{P}_v = \frac{\partial f_v}{\partial \hat{X}_v} P_v + P_v \frac{\partial f_v^T}{\partial \hat{X}_v} + G_v Q_v G_v^T - P_v H_v^T R_v^{-1} H_v P_v, \tag{13b}$$

and

$$R_v = cov\left(\eta_{X_v}\right), Q_v = diag(cov\left(\xi_{q_v}\right), cov\left(\xi_{\dot{q}_v}\right), cov\left(\xi_{\theta_v}\right), cov\left(\xi_{v_{v_v}}\right), cov\left(\xi_{v_{c_v}}\right), cov\left({}^0\xi_{T_{ve}}\right)),$$

$$f_v\left(\hat{X}_v, T_v\right) = \begin{bmatrix} \dot{\hat{q}}_v \\ \ddot{\hat{q}}_v \\ \dot{\hat{\theta}}_v \\ \dot{\hat{v}}_{v_v} \\ \dot{\hat{v}}_{c_v} \\ \dot{\hat{T}}_{ve} \end{bmatrix} = \begin{bmatrix} \dot{\hat{q}}_v \\ \hat{M}_v^{-1}\left(-\hat{V}_v \dot{\hat{q}}_v - \hat{g}_v + T_v - \hat{T}_{ve} - \hat{T}_{vf}\right) \\ 0 \\ 0 \\ 0 \\ 0 \end{bmatrix}, \tag{14a}$$

where $\hat{}$ means the corresponding estimated item, $cov\left(\xi_{q_v}\right)$, $cov\left(\xi_{\dot{q}_v}\right)$, $cov\left(\xi_{\theta_v}\right)$, $cov\left(\xi_{v_{v_v}}\right)$, $cov\left(\xi_{v_{c_v}}\right)$, $cov\left({}^0\xi_{T_{ve}}\right)$ and $cov\left(\eta_v\right)$ are, respectively, the covariance matrices of the input stochastic, zero mean, and Gaussian noises ξ_{q_v}, $\xi_{\dot{q}_v}$, ξ_{θ_v}, $\xi_{v_{v_v}}$, $\xi_{v_{c_v}}$, ${}^0\xi_{T_{ve}}$, and the output stochastic, zero mean, and Gaussian noise η_{X_v}, and

$$F_v(t) = \frac{\partial f_v}{\partial \hat{X}_v} = \begin{bmatrix} 0 & I & 0 & 0 & 0 & 0 \\ F_{v21}(t) & F_{v22}(t) & F_{v23}(t) & F_{v24}(t) & F_{v25}(t) & F_{v26}(t) \\ 0 & 0 & 0 & 0 & 0 & 0 \\ 0 & 0 & 0 & 0 & 0 & 0 \\ 0 & 0 & 0 & 0 & 0 & 0 \\ 0 & 0 & 0 & 0 & 0 & 0 \end{bmatrix} \tag{14b}$$

where

$$F_{v21}(t) = -\hat{M}_v^{-1}\left(\frac{\partial \hat{M}_v}{\partial \hat{q}_v}\ddot{\hat{q}}_v + \frac{\partial \hat{V}_v \dot{\hat{q}}_v}{\partial \hat{q}_v} + \frac{\partial \hat{g}_v}{\partial \hat{q}_v} + \frac{\partial \hat{T}_{fv}}{\partial \hat{q}_v}\right),$$

$$F_{v22}(t) = -\hat{M}_v^{-1}\left(\frac{\partial \hat{V}_v \dot{\hat{q}}_v}{\partial \dot{\hat{q}}_v} + \frac{\partial \hat{T}_{fv}}{\partial \dot{\hat{q}}_v}\right),$$

$$F_{v23}(t) = -\hat{M}_v^{-1}\left(\frac{\partial \hat{M}_v}{\partial \hat{\theta}_v}\ddot{\hat{q}}_v + \frac{\partial \hat{V}_v \dot{\hat{q}}_v}{\partial \hat{\theta}_v} + \frac{\partial \hat{g}_v}{\partial \hat{\theta}_v}\right),$$

$$F_{v24}(t) = -\hat{M}_v^{-1}\frac{\partial \hat{T}_{fv}}{\partial \dot{\hat{v}}_{v_v}}, F_{v25}(t) - \hat{M}_v^{-1}\frac{\partial \hat{T}_{fv}}{\partial \dot{\hat{v}}_{c_v}},$$

$$F_{v26}(t) = -\hat{M}_v^{-1}.$$

It is easy to see that the relation between $\hat{T}_{ve}$ and $\hat{T}_e$ is

$$\hat{T}_{ve} = \hat{T}_e e^{t_1 s}. \tag{15}$$

Based on the Theorem 1 in [15], the IEAOB is asymptotically stable and can accurately identify the VIM, the estimated states $\hat{X}_v$ asymptotically converge to the real values X_v, accordingly one can get $\hat{G}_s(s) = G_s(s)$.

2) ESTIMATION OF ROUND-TRIP DELAY WITH PADÉ APPROXIMATION AND ACTIVE OBSERVER

In order to obtain the round-trip delay for the ASP, the Padé approximation in [35] is utilized to model the round-trip time-varying delay t as follows:

$$e^{-ts} \approx \frac{\sum_{k=0}^{n}(-1)^k c_k t^k s^k}{\sum_{k=0}^{n} c_k t^k s^k}, \tag{16}$$

where

$$c_k = \frac{(2n-k)!n!}{2n!k!(n-k)!}, k = 0, 1, 2, \ldots, n.$$

Let's make the inverse Laplace transform of (16) and one can get:

$$c_n t^n y^{(n)} + \cdots + c_1 t y^{(1)} + c_0 y = (-1)^n c_n t^n u^{(n)} + \cdots - c_1 t u^{(1)} + c_0 u, \tag{17}$$

and its state-space equation can be written as

$$\begin{cases} \dot{X} = AX + BU \\ Y = CX + DU \end{cases} \tag{18}$$

where

$$A = \begin{bmatrix} 0 & 1 & 0 & & \cdots & 0 \\ 0 & 0 & 1 & & & 0 \\ & & \vdots & & \ddots & \vdots \\ 0 & 0 & 0 & & \cdots & 1 \\ -\frac{c_0}{c_n t^n} & -\frac{c_1}{c_n t^{n-1}} & -\frac{c_2}{c_n t^{n-2}} & & \cdots & -\frac{c_{n-1}}{c_n t} \end{bmatrix},$$

$$B = \begin{bmatrix} 0 \\ \vdots \\ 0 \\ 1 \end{bmatrix}, C^T = \begin{bmatrix} \frac{c_0}{c_n t^n} - (-1)^n \frac{c_0}{c_n t^n} \\ -\frac{c_1}{c_n t^{n-1}} - (-1)^n \frac{c_1}{c_n t^{n-1}} \\ \cdots \\ (-1)^{n-1}\frac{c_{n-1}}{c_n t} - (-1)^n \frac{c_{n-1}}{c_n t} \end{bmatrix},$$

$$D = (-1)^n.$$

Using this system to estimate the time delay, we have to add another system state p_k into the state X to model the time delay t with $p_k = t$.

In this work, the active observer in [14] and [16] is employed to estimate the time delay. The active observer concept relies on adopting an extra relationship (auxiliary input) to estimate the time delay referred to as the system input. The extra state p_k describing the time delay is modelled as a random walk process (a Gauss-Markov chain) and defined by

$$p_k = \sum_{j=1}^{S} (-1)^{j+1} \frac{S!}{j!\,(S-j)!} p_{k-j} + {}^{S-1}\xi_{p_k}, \tag{19}$$

where the Sth-order derivative of p_k is randomly distributed. ${}^{S-1}\xi_{p_k}$ is a Gaussian variable with zero mean.

When S=1, the active observer for the state x_k,p_k can be formulated as

$$\begin{bmatrix} \hat{x}_{k+1} \\ \hat{p}_{k+1} \end{bmatrix} = \begin{bmatrix} AB \\ 01 \end{bmatrix} \begin{bmatrix} \hat{x}_k \\ \hat{p}_k \end{bmatrix} + \begin{bmatrix} B \\ 0 \end{bmatrix} U_k + L \left(Y_k - [C0] \begin{bmatrix} \hat{x}_k \\ \hat{p}_k \end{bmatrix} - \begin{bmatrix} D \\ 0 \end{bmatrix} U_k \right), \tag{20}$$

where L represents the observer gain.

C. IEAOB FOR MASTER/SLAVE MODEL IDENTIFICATION AND EXTERNAL FORCE ESTIMATION

Let's recall the dynamical model for master and slave robots in (3), the IEAOB [15] is designed as follows:

$$\dot{\hat{X}}_* = f_* \left(\hat{X}_*, T_* \right) + P_* H_*^T R_*^{-1} \left(Y_* - H_* \hat{X}_* \right), \tag{21a}$$

where

$$\begin{aligned} \dot{P}_* &= \frac{\partial f_*}{\partial \hat{X}_*} P_* + P_* \frac{\partial f_*^T}{\partial \hat{X}_*} + G_* Q_* G_*^T - P_* H_*^T R_*^{-1} H_* P_*, \\ R_* &= cov\left(\eta_{X_*}\right), Q_* = diag(cov\left(\xi_{q_*}\right), cov\left(\xi_{\dot{q}_*}\right), \\ &\quad cov\left(\xi_{\theta_*}\right), cov\left(\xi_{v_{v_*}}\right), cov\left(\xi_{v_{c_*}}\right), cov\left({}^0\xi_{T_{h/e}}\right)), \\ f_*\left(\hat{X}_*, T_*\right) &= \begin{bmatrix} \dot{\hat{q}}_* \\ \ddot{\hat{q}}_* \\ \dot{\hat{\theta}}_* \\ \dot{\hat{v}}_{v_*} \\ \dot{\hat{v}}_{c_*} \\ \dot{\hat{T}}_{\frac{h}{e}} \end{bmatrix} \\ &= \begin{bmatrix} \dot{\hat{q}}_* \\ \hat{M}_*^{-1} \left(-\hat{V}_* \dot{\hat{q}}_* - \hat{g}_* + T_* \pm \hat{T}_{h/e} - \hat{T}_{f_*} \right) \\ 0 \\ 0 \\ 0 \\ 0 \end{bmatrix}, \end{aligned} \tag{22a}$$

where $* = m/s$,$\hat{}$ means the estimated item,$cov\left(\xi_{q_*}\right)$, $cov\left(\xi_{\dot{q}_*}\right)$, $cov\left(\xi_{\theta_*}\right)$, $cov\left(\xi_{v_{v_*}}\right)$, $cov\left(\xi_{v_{c_*}}\right)$, $cov\left({}^0\xi_{T_{h/e}}\right)$, and $cov\left(\eta_*\right)$ are, respectively, the covariance matrices of the input stochastic, zero mean, and Gaussian noises ξ_{q_*}, $\xi_{\dot{q}_*}$, ξ_{θ_*}, $\xi_{v_{v_*}}$, $\xi_{v_{c_*}}$, ${}^0\xi_{T_{h/e}}$, and output stochastic, zero mean, and Gaussian noise η_{X_*}, and

$$\begin{aligned} F_*(t) &= \frac{\partial f_*}{\partial \hat{X}_*} \\ &= \begin{bmatrix} 0 & I & 0 & 0 & 0 & 0 \\ F_{*21}(t) & F_{*22}(t) & F_{*23}(t) & F_{*24}(t) & F_{*25}(t) & F_{*26}(t) \\ 0 & 0 & 0 & 0 & 0 & 0 \\ 0 & 0 & 0 & 0 & 0 & 0 \\ 0 & 0 & 0 & 0 & 0 & 0 \\ 0 & 0 & 0 & 0 & 0 & 0 \end{bmatrix} \end{aligned} \tag{22b}$$

where

$$\begin{aligned} F_{*21}(t) &= -\hat{M}_*^{-1} \left(\frac{\partial \hat{M}_*}{\partial \hat{q}_*} \ddot{\hat{q}}_* + \frac{\partial \hat{V}_* \dot{\hat{q}}_*}{\partial \hat{q}_*} + \frac{\partial \hat{g}_*}{\partial \hat{q}_*} + \frac{\partial \hat{T}_{f_*}}{\partial \hat{q}_*} \right), \\ F_{*22}(t) &= -\hat{M}_*^{-1} \left(\frac{\partial \hat{V}_* \dot{\hat{q}}_*}{\partial \dot{\hat{q}}_*} + \frac{\partial \hat{T}_{f_*}}{\partial \dot{\hat{q}}_*} \right), \\ F_{*23}(t) &= -\hat{M}_*^{-1} \left(\frac{\partial \hat{M}_*}{\partial \hat{\theta}_*} \ddot{\hat{q}}_* + \frac{\partial \hat{V}_* \dot{\hat{q}}_*}{\partial \hat{\theta}_*} + \frac{\partial \hat{g}_*}{\partial \hat{\theta}_*} \right), \\ F_{*24}(t) &= -\hat{M}_*^{-1} \frac{\partial \hat{T}_{f_*}}{\partial \dot{\hat{v}}_{v_*}}, F_{*25}(t) = -\hat{M}_*^{-1} \frac{\partial \hat{T}_{f_*}}{\partial \dot{\hat{v}}_{c_*}}, \\ F_{*26}(t) &= \pm \hat{M}_*^{-1}. \end{aligned}$$

Then, one has

$$\hat{T}_{f_*} = \hat{v}_{c_*} sgn\left(\dot{\hat{q}}_*\right) + \hat{v}_{v_*} \dot{\hat{q}}_*. \tag{23}$$

With the estimated robot models and the control design in the above subsections, the controllers for the master and slave manipulators are developed as follows:

$$\begin{aligned} T_m &= C_f(s) * \left(\hat{T}_h - \hat{T}_e e^{-t_2 s} - \hat{T}_{ve} \left(1 - e^{-\hat{t}s} \right) \right) - \hat{T}_h \\ &\quad + \hat{T}_{f_m} + \hat{g}_m \left(\hat{q}_m, \hat{\theta}_m \right); \end{aligned} \tag{24a}$$

$$T_s = C_p(s) * \left(\hat{q}_m e^{-t_1 s} - \hat{q}_s \right) + \hat{T}_e + \hat{T}_{f_s} + \hat{g}_s \left(\hat{q}_s, \hat{\theta}_s \right); \tag{24b}$$

where $C_f(s)$,$C_p(s)$ are the force controller and position controller, respectively, and the

$$C_f(s) = K_f, C_p(s) = K_v s + K_p \tag{25}$$

D. STABILITY ANALYSIS

In this work, the human and environment for the stability analysis are modeled as [8]:

$$T_h(t) = -\emptyset_m \left(\dot{q}_m(t) + \rho q_m(t) \right), \tag{26a}$$

$$T_e(t) = \emptyset_s \left(\dot{q}_s(t) + \rho q_s(t) \right), \tag{26b}$$

where ρ, $\emptyset_m$ and $\emptyset_s$ are positive constant matrices and are properties of the human and the environment, respectively.

Theorem 1: In the teleoperation system described by equation (1) with the control laws (24) and the IEAOB (13), (21) and the ASP (7), when the human and environmental forces satisfy (26), the velocities $\dot{q}_m(t)$, $\dot{q}_s(t)$ and position errors are bounded, provided that

1) K_v, K_p, and K_f are bounded and positive definite matrices,

2) T_h, T_e are bounded and continuous,

3) $\alpha_1 I \leq Q_m(t) \leq \alpha_2 I$, $\beta_1 I \leq Q_s(t) \leq \beta_2 I$, $\gamma_1 I \leq Q_v(t) \leq \gamma_2 I$,

4) $\alpha_3 I \leq R_m(t) \leq \alpha_4 I$, $\beta_3 I \leq R_s(t) \leq \beta_4 I$, $\gamma_3 I \leq R_v(t) \leq \gamma_4 I$,

5) The following is true:

$$\alpha_5 I \leq \int_t^{t+\sigma} \left[F_{m23}(\tau) \;\; F_{m24}(\tau) \; F_{m25}(\tau) \; F_{m26}(\tau) \right]^T * \left[F_{m23}(\tau) \;\; F_{m24}(\tau) \; F_{m25}(\tau) \; F_{m26}(\tau) \right] d\tau \leq \alpha_6 I,$$

where $F_{m23}(\tau)$, $F_{m24}(\tau)$, $F_{m25}(\tau)$ and $F_{m26}(\tau)$ are evaluated along $\hat{X}_m$ and $\dot{F}_{m23}(\tau)$, $\dot{F}_{m24}(\tau)$, $\dot{F}_{m25}(\tau)$ and $\dot{F}_{m26}(\tau)$ are bounded, with

$$F_{m23}(t) = -\hat{M}_m^{-1}\left(\frac{\partial \hat{M}_m}{\partial \hat{\theta}_m}\ddot{q}_m + \frac{\partial \hat{V}_m \dot{\hat{q}}_m}{\partial \hat{\theta}_m} + \frac{\partial \hat{g}_m}{\partial \hat{\theta}_m}\right),$$

$$F_{m24}(t) = -\hat{M}_m^{-1}\frac{\partial \hat{T}_{f_m}}{\partial \dot{\hat{v}}_{v_m}}, F_{m25}(t) = -\hat{M}_m^{-1}\frac{\partial \hat{T}_{f_m}}{\partial \dot{\hat{v}}_{c_m}},$$

$$F_{m26}(t) = \hat{M}_m^{-1},$$

for some positive constants $\alpha_1, \alpha_2, \alpha_3, \alpha_4, \alpha_5, \alpha_6, \sigma$ and all $t > t_0$,

6) The following is true:

$$\beta_5 I \leq \int_t^{t+\sigma} \left[F_{s23}(\tau) \;\; F_{s24}(\tau) \; F_{s25}(\tau) \; F_{s26}(\tau) \right]^T * \left[F_{s23}(\tau) \;\; F_{s24}(\tau) \; F_{s25}(\tau) \; F_{s26}(\tau) \right] d\tau \leq \beta_6 I,$$

where $F_{s23}(\tau)$, $F_{s24}(\tau)$, $F_{s25}(\tau)$ and $F_{s26}(\tau)$ are evaluated along $\hat{X}_s$ and $\dot{F}_{s23}(\tau)$, $\dot{F}_{s24}(\tau)$, $\dot{F}_{s25}(\tau)$ and $\dot{F}_{s26}(\tau)$ are bounded, with

$$F_{s23}(t) = -\hat{M}_s^{-1}\left(\frac{\partial \hat{M}_s}{\partial \hat{\theta}_s}\ddot{\hat{q}}_s + \frac{\partial \hat{V}_s \dot{\hat{q}}_s}{\partial \hat{\theta}_s} + \frac{\partial \hat{g}_s}{\partial \hat{\theta}_s}\right),$$

$$F_{s24}(t) = -\hat{M}_s^{-1}\frac{\partial \hat{T}_{f_s}}{\partial \dot{\hat{v}}_{v_s}}, F_{s25}(t) = -\hat{M}_s^{-1}\frac{\partial \hat{T}_{f_s}}{\partial \dot{\hat{v}}_{c_s}},$$

$$F_{s26}(t) = -\hat{M}_s^{-1},$$

for some positive constants $\beta_1, \beta_2, \beta_3, \beta_4, \beta_5, \beta_6, \sigma$ and all $t > t_0$.

7) The following is true:

$$\gamma_5 I \leq \int_t^{t+\sigma} \left[F_{v23}(\tau) \;\; F_{v24}(\tau) \;\; F_{v25}(\tau) \; F_{v26}(\tau) \right]^T * \left[F_{v23}(\tau) \;\; F_{v24}(\tau) \;\; F_{v25}(\tau) \; F_{v26}(\tau) \right] d\tau \leq \gamma_6 I,$$

where $F_{v23}(\tau)$, $F_{v24}(\tau)$, $F_{v25}(\tau)$, and$F_{v26}(\tau)$ are evaluated along $\hat{X}_v$ and $\dot{F}_{v23}(\tau)$, $\dot{F}_{v24}(\tau)$, $\dot{F}_{v25}(\tau)$, and$\dot{F}_{v26}(\tau)$ are bounded, with

$$F_{v23}(t) = -\hat{M}_v^{-1}\left(\frac{\partial \hat{M}_v}{\partial \hat{\theta}_v}\ddot{\hat{q}}_v + \frac{\partial \hat{V}_v \dot{\hat{q}}_v}{\partial \hat{\theta}_v} + \frac{\partial \hat{g}_v}{\partial \hat{\theta}_v}\right),$$

$$F_{v24}(t) = -\hat{M}_v^{-1}\frac{\partial \hat{T}_{f_v}}{\partial \dot{\hat{v}}_{v_v}}, F_{v25}(t) = -\hat{M}_v^{-1}\frac{\partial \hat{T}_{f_v}}{\partial \dot{\hat{v}}_{c_v}},$$

$$F_{v26}(t) = -\hat{M}_v^{-1},$$

for some positive constants $\gamma_1, \gamma_2, \gamma_3, \gamma_4, \gamma_5, \gamma_6, \sigma$ and all $t > t_0$.

Proof: The stability issue of the bilateral teleoperation systems originates from time delay in the communication channels, which is an inherent property often occurring in the distant transmission for teleoperation systems and may destabilize the system. Through the design of the ASP with IEAOB, Padé approximation and the active observer, the stability issue caused by communication time delay is well addressed. Now we only need to separately consider the stabilities at master and slave sides with the proposed control architecture.

Define

$$e_f = T_h - T_e e^{t_1 s}, e_s = q_s - q_m e^{-t_1 s}, \tilde{\ddot{q}}_* = \ddot{q}_* - \hat{\ddot{q}}_*,$$
$$\tilde{\dot{q}}_* = \dot{q}_* - \hat{\dot{q}}_*, \tilde{q}_* = q_* - \hat{q}_*, \tilde{\theta}_* = \theta_* - \hat{\theta}_*,$$
$$\tilde{v}_{v_*} = v_{v_*} - \hat{v}_{v_*}, \tilde{v}_{c_*} = v_{c_*} - \hat{v}_{c_*}, \tilde{T}_{h/e} = T_{h/e} - \hat{T}_{h/e},$$

where $* = m, v, s$. If conditions 3,4,5,6,7 of the Theorem are satisfied, according to Theorem 1 in [15], $\tilde{q}_m, \tilde{\dot{q}}_m, \tilde{\theta}_m, \tilde{v}_{v_m}, \tilde{v}_{c_m}, \tilde{T}_h, \tilde{q}_s, \tilde{\dot{q}}_s, \tilde{\theta}_s, \tilde{v}_{v_s}, \tilde{v}_{c_s}, \tilde{T}_e \in L_2 \cap L_\infty$.

1) We first consider the master side, and show $\ddot{q}_m, \dot{q}_m, e_f \in L_2 \cap L_\infty$ under the proposed controller (24a).

Combining the master dynamical model in (1) and the controller in (24a), the master system can be changed to

$$\begin{aligned} T_m &= M_m(q_m, \theta_m)\ddot{q}_m + V_m(q_m, \dot{q}_m, \theta_m)\dot{q}_m + g_m(q_m, \theta_m) \\ &\quad + T_{f_m} - T_h \\ &= C_f(s) * \left(\hat{T}_h - \hat{T}_e e^{t_1 s}\right) - \hat{T}_h + \hat{T}_{f_m} + \hat{g}_m\left(\hat{q}_m, \hat{\theta}_m\right), \end{aligned} \tag{27}$$

Then, one can get

$$\begin{aligned} &M_m(q_m, \theta_m)\ddot{q}_m + V_m(q_m, \dot{q}_m, \theta_m)\dot{q}_m \\ &\quad = K_f * e_f + \tilde{T}_h - \tilde{T}_{f_m} - \tilde{g}_m\left(\tilde{q}_m, \tilde{\theta}_m\right). \end{aligned} \tag{28}$$

Because $\tilde{q}_m, \tilde{\dot{q}}_m, \tilde{\theta}_m, \tilde{T}_h, \tilde{v}_{v_s}, \tilde{v}_{c_s} \in L_2 \cap L_\infty$, we have $\tilde{T}_{f_m} \in L_2 \cap L_\infty$, $\tilde{g}_m\left(\tilde{q}_m, \tilde{\theta}_m\right) \in L_2 \cap L_\infty$.

Now, if condition 2 of the Theorem is satisfied, according to (26a) and (6), we have $\dot{q}_m \in L_2 \cap L_\infty$, and because $\ddot{q}_m$ is uniformly continuous ($\int_0^t \ddot{q}_m(\eta)\, d\eta = \dot{q}_m(t) - \dot{q}_m(0)$), it can be concluded that $\ddot{q}_m \in L_2 \cap L_\infty$ based on Barbălat's Lemma.

According to Property 1 and Property 2 in (4) and (5), we have

$$\begin{aligned} &M_m(q_m, \theta_m)\ddot{q}_m + V_m(q_m, \dot{q}_m, \theta_m)\dot{q}_m \\ &\quad \leq \sigma_{max}(M_m(q_m))\ddot{q}_m + Z\|\dot{q}_m(t)\|_2^2 \in L_2 \cap L_\infty. \end{aligned}$$

As the time delay T_1, T_2 are assumed to be bounded and if the conditions 1 of the Theorem are satisfied, we have $\hat{T}_h - \hat{T}_e e^{t_1 s} \in L_2 \cap L_\infty$. Hence,

$$\begin{aligned} e_f &= T_h - T_e e^{t_1 s} \\ &= \hat{T}_h - \hat{T}_e e^{t_1 s} + \tilde{T}_h - \tilde{T}_e e^{t_1 s} \in L_2 \cap L_\infty. \end{aligned} \tag{29}$$

Furthermore, we can conclude that from (26) and (30) the force tracking error $e_f \in L_2 \cap L_\infty$.

2) Similarly, we can consider the slave side, and show that $\dot{q}_s, \ddot{q}_s, e_s = q_s - q_m e^{-t_1 s} \in L_2 \cap L_\infty$ according to the procedure in 1).

Therefore, the entire teleoperation system is proved to be stable with the proposed teleoperation system.

E. SLIDING MODE CONTROL FOR FURTHER TIME DELAY EFFECT SUPPRESSION

In practice, there are some constraints for the round-trip delay estimation with Padé approximation and the active observer in Subsection 3.B.2. For example, the round-trip delay should have an upper and lower limit. The smallest time delay should be bigger than the sampling time. The accuracy of the estimation depends on the order of the Padé approximation. In addition, the sampling time needs to be chosen small enough so that this inaccuracy is small. Based on this knowledge, one can get the round-trip time delay estimation $\hat{t}$ based on Padé approximation and the active observer can obtain a reasonable result, but cannot represent the actual value $(t_1 + t_2)$, i.e., there is a small estimation error $e_t = t(t) - \hat{t}(t)$.

Due to the imperfect estimation of the round-trip delay, the time delay effect cannot be compensated for with the ASP, which could cause perturbations and reduce the system transparency. Hence, a sliding mode control algorithm at the master side is proposed in this Subsection for further suppression.

Let's reconsider the dynamical model in (1a), and put (15) and (24a) into (1a), the dynamical model can be re-written as

$$\begin{aligned} &M_m(q_m, \theta_m)\ddot{q}_m + V_m(q_m, \dot{q}_m, \theta_m)\dot{q}_m + g_m(q_m, \theta_m) + T_{f_m} \\ &= C_f(s) * \left(\hat{T}_h - \hat{T}_e e^{-t_2 s} - \hat{T}_e e^{t_1 s}\left(1 - e^{-\hat{t}s}\right)\right) - \hat{T}_h + T_h \\ &\quad + \hat{T}_{f_m} + \hat{g}_m\left(\hat{q}_m, \hat{\theta}_m\right), \end{aligned} \tag{30}$$

According to the Theorem 1 in [15], (30) can be further written as

$$\begin{aligned} &M_m(q_m, \theta_m)\ddot{q}_m + V_m(q_m, \dot{q}_m, \theta_m)\dot{q}_m \\ &\quad = K_f * (\hat{T}_h - \hat{T}_e e^{t_1 s} + d) \end{aligned} \tag{31}$$

where $d = \hat{T}_e * (e^{-(\hat{t}-t_1)s} - e^{-t_2 s})$ is the perturbation resulting from the time delay due to the imperfect estimation of the round-trip delay by the ASP.

By adding the sliding model compensation term $T_{sliding}$ into (31), the dynamical model becomes

$$\begin{aligned} &M_m(q_m, \theta_m)\ddot{q}_m + V_m(q_m, \dot{q}_m, \theta_m)\dot{q}_m \\ &\quad = K_f * (\hat{T}_h - \hat{T}_{ve} + d + T_{sliding}). \end{aligned} \tag{32}$$

The aim is to design the sliding mode compensation term $T_{sliding}$ to omit d. The proposed algorithm sets the sliding surface as:

$$\begin{aligned} \sigma = \int_0^t \Bigg(&\frac{M_m(q_m, \theta_m)\ddot{q}_m + V_m(q_m, \dot{q}_m, \theta_m)\dot{q}_m}{K_f} \\ &- \hat{T}_h + \hat{T}_{ve} \Bigg) d\eta. \end{aligned} \tag{33}$$

Based on (33), if the sliding surface σ converges to zero, the perturbation term d can be compensated for by $T_{sliding}$. Build a Lyapunov function for the sliding mode controller as

$$V = \sigma^T \sigma. \tag{34}$$

Therefore, the derivative of (34) will result in:

$$\dot{V} = (T_{sliding} + d)^T \sigma + \sigma^T \left(T_{sliding} + d\right). \tag{35}$$

The sliding control input is designed as:

$$T_{sliding} = -K_l \sigma - K_s sgn(\sigma) \tag{36}$$

where $sgn()$ is the standard signum function, $K_l, K_s > 0$, the term K_l in control removes chatter and makes it smooth.

Based on (35) and (36), by tuning K_l and K_s to large values, $\dot{V}$ is negative semi-definite and σ will converge to zero. The proposed sliding control in (36) will omit the perturbation and enhance the system transparency.

IV. EXPERIMENT STUDY

A. EXPERIMENTAL SET-UP

The experiments are performed on two Phantom manipulators: Phantom Omni and Phantom Desktop (Sensable Technologies, Inc., Wilmington, MA) as shown in Figure 3. PhanTorque toolkit is applied by two computers to control the two robots. The PhanTorque toolkit enables the users to work with the Sensable Phantom haptic devices in the Matlab/Simulink environment quickly and easily. In this experiment, only the first actuated joints of the Omni and desktop robots are used while the second and third actuated joints are locked at zero. The manipulator motion of the first joint is governed as follows:

$$M_* \ddot{q}_* + T_{f_*} = T_* \pm T_{h/e}, \tag{37}$$

where $* = m/s$, M_* is a moment of inertia, T_{f_*} is the friction torque calculated in (2), and T_* is a torque which the motor generates. The angle of the manipulator is measured by an encoder with resolution of 0.055 mm. The sample time in the experiment is set to 1.0 ms. The actual values of the robot dynamical parameter and friction coefficients are $M_{m/s} = 5.0\text{x}10^{-3} kgm^2$, $v_{v_{m/s}} = -1.5\text{x}10^{-3}$, $v_{c_{m/s}} = 1.0\text{x}10^{-3}$. The time-varying delays are simulated in PC. The forward and feedback time delays are chosen as random variables with a uniform distribution over [0.04, 0.2] s. The random nature of these time delays makes it possible to show the effectiveness of the proposed method for varying time delays. In the experiments, human operator manipulates the master manipulator and the slave manipulator makes contact with the environment at around 0.25 rad.

In order to demonstrate the superiority of the proposed approach, we assume that there is no parameter variation (M_m, v_{v_m}, v_{c_m} are set to the actual values) for the master robot, while 20% parameter variation (M_s, v_{v_s}, v_{c_s} are 20% smaller than the actual values) is considered in slave robot. Three approaches are implemented for fair comparison, as shown in the following:

FIGURE 3. Experiment set-up for teleoperation experiment.

A1: The robust adaptive observer-based predictive control proposed in this paper to improve the transparency performance of both position tracking and force feedback for nonlinear teleoperation manipulators. The parameters of the PD position controllers are selected as $K_p = 0.5$ and $K_v = 5$. The parameters of the P force controllers are selected as $K_f = 0.8$. The parameters for the sliding mode controller are chosen as $K_l = 1.2, K_s = 1.2$. From filtering theory, the initial filtered state estimates are the expected values of these states at the beginning of control. Hence, for the robotic manipulator starting at rest and at origin, the initial filtered states: $q_{m_0} = 0, q_{s_0} = 0, \dot{q}_{m_0} = 0, \dot{q}_{s_0} = 0$. Hence, the initial conditions of IEAOB for master robot, slave robot and VIM are chosen respectively as

$$
\begin{aligned}
\hat{X}_{m_0} &= \left(0, 0, 5.0\text{x}10^{-3}, -1.5\text{x}10^{-3}, 1.0\text{x}10^{-3}, 0\right)', \\
R_m &= 1.0\text{x}10^{-4}, \\
Q_m &= diag\{1.0\text{x}10^{-7}, 1.0\text{x}10^{-7}, 1.0\text{x}10^{-7}, \\
&\quad 1.0\text{x}10^{-7}, 1.0\text{x}10^{-7}, 1.0\text{x}10^{-6}, \} \\
P_{m_0} &= diag\{1.0\text{x}10^{-6}, 1.0\text{x}10^{-6}, 1.0\text{x}10^{-6}, \\
&\quad 1.0\text{x}10^{-6}, 1.0\text{x}10^{-6}, 1.0\text{x}10^{-4}.\} \\
\hat{X}_{s_0} &= (0, 0, 4.0\text{x}10^{-3}, -1.2\text{x}10^{-3}, 0.8\text{x}10^{-3}, 0)', \\
R_s &= 1.0\text{x}10^{-4}, \\
Q_s &= diag\{1.0\text{x}10^{-7}, 1.0\text{x}10^{-7}, 1.0\text{x}10^{-7}, \\
&\quad 1.0\text{x}10^{-7}, 1.0\text{x}10^{-7}, 1.0\text{x}10^{-6}, \} \\
P_{s_0} &= diag\{1.0\text{x}10^{-6}, 1.0\text{x}10^{-6}, 1.0\text{x}10^{-6}, \\
&\quad 1.0\text{x}10^{-6}, 1.0\text{x}10^{-6}, 1.0\text{x}10^{-4}.\} \\
\hat{X}_{v_0} &= (0, 0, 4.0\text{x}10^{-3}, -1.2\text{x}10^{-3}, 0.8\text{x}10^{-3}, 0)', \\
R_v &= 1.0\text{x}10^{-4}, \\
Q_v &= diag\{1.0\text{x}10^{-7}, 1.0\text{x}10^{-7}, 1.0\text{x}10^{-7}, \\
&\quad 1.0\text{x}10^{-7}, 1.0\text{x}10^{-7}, 1.0\text{x}10^{-6}, \} \\
P_{v_0} &= diag\{1.0\text{x}10^{-6}, 1.0\text{x}10^{-6}, 1.0\text{x}10^{-6}, \\
&\quad 1.0\text{x}10^{-6}, 1.0\text{x}10^{-6}, 1.0\text{x}10^{-4}.\}
\end{aligned}
$$

In this experiment, time delay is modelled as two order Padé approximation, and the first order AOB is used to estimate the delay. The specific condition of AOB is chosen as

$$
\begin{aligned}
\hat{X}_{t_0} &= (0, 0, 0)', R_t = 1.0\text{x}10^{-4}, \\
Q_t &= diag\{1.0\text{x}10^{-7}, 1.0\text{x}10^{-7}, 1.0\text{x}10^{-6}, \} \\
P_{t_0} &= diag\{1.0\text{x}10^{-6}, 1.0\text{x}10^{-6}, 1.0\text{x}10^{-4}.\}
\end{aligned}
$$

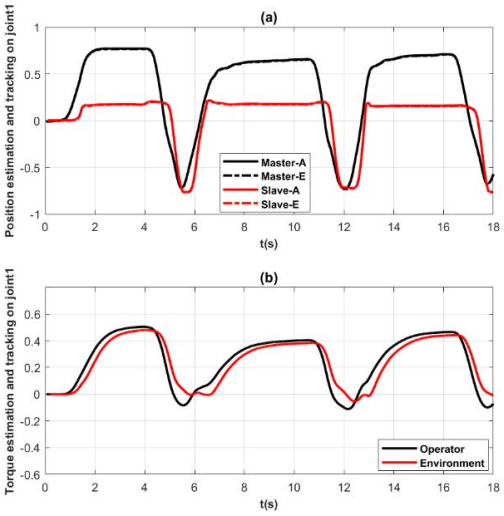

FIGURE 4. Experimental results with the proposed teleoperation approach A1 (a) Position response. (b) Force response.

A2: The Smith predictor-based control in [13] to achieve stability under time delay. The disturbance observer (DOB) cut-off frequency is chosen as $g_d = 25 rad/s$, and the reaction torque observer (RTOB) cut-off frequency is chosen as $g_{reac} = 50 rad/s$. The parameters of the PD position controllers are selected as $K_p = 0.5$ and $K_v = 5$. The parameters of the P force controllers are selected as $K_f = 0.8$.

A3: The neural network-based control in [27] for enhanced position and force tracking performance in the presence of time delay. The selection of the parameters can refer to [27], specifically, $k_{mv} = k_{sv} = 50, \Gamma_m = \Gamma_s = 2.5$, $k_m = k_s = 0.01, \Lambda_m = \Lambda_s = 5, \gamma_{mN} = \gamma_{sN} = 0.3, b_{md} = b_{sd} = 0.2, D_d = 1.8, C_d = 0, G_d = 19.6, E_m = E_s = 0.1 * \begin{bmatrix} -1.5 & -1 & -0.5 & 0 & 0.5 & 1 & 1.5 \end{bmatrix}_{5x7}$.

B. EXPERIMENT RESULTS

Figure 4a, 7a and 8a show the position tracking and estimation performance for three approaches, respectively. Figure 4a depicts the performance of the proposed approach A1. As expected, the actual position tracks the desired position when in free motion at around [0s, 1.5s], [4.2s, 6.3s], [11s, 12.9s] and [16.5s, 18s], but not when in contact with the environment. Meanwhile, the estimated position obtained by IEAOB matches the actual position. Figure 7a shows that the Smith predictor-based approach A2 can only attain approximate position tracking during free motion at [0s, 0.7s], [3.4s, 6.4s], [8.9s, 11.7s] and [14.3s, 18s], but there is still some chattering during the tracking process. Meanwhile, Figure 8a illustrates the position estimation and tracking performance of the neural network-based approach A3. As observed in Figure 8a, the position tracking happens during free motion at around [0s, 1.3 s], [5.4s, 7.1s], [10.3s, 12.5s], and [15.6s, 18 s], it is noticed that during the initial moment the transient tracking performance is a little bit slow due to the neural network online weight training for the approach A3, there is also

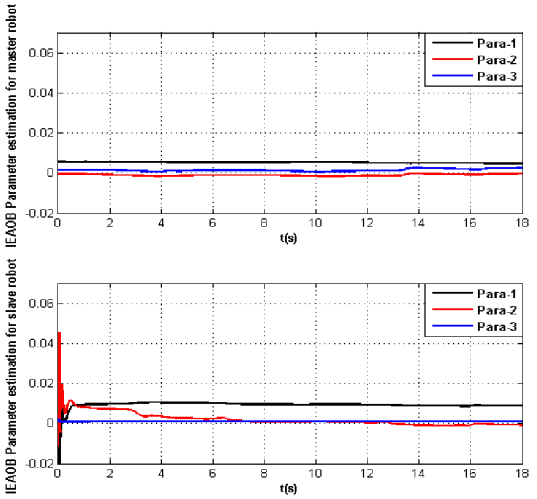

FIGURE 5. Parameter and friction estimation performance of IEAOB for the master and slave robots (Para-1 represents $M_{m/s}$, Para-2 represents $v_{v_{m/s}}$, Para-3 represents $v_{c_{m/s}}$.)

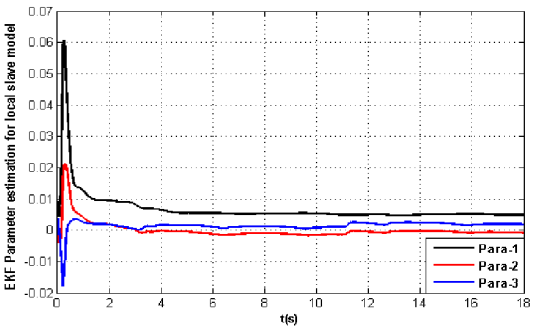

FIGURE 6. Parameter and friction estimation performance of IEAOB for VIM (Para-1 represents M_v, Para-2 represents v_{v_v}, Para-3 represents v_{c_v}.)

some chartering during the experiment because the online weight updating laws based on the control errors sometimes would suffer from the parameter drifting issue when a high gain adaptation is used. The force tracking performances for three approaches are given in Figures 4b, 7b and 8b, respectively. The torques are estimated when the robot is in contact with the environment. As illustrated in Figure 4b for the proposed approach A1, when the position of the end effector does not follow the desired position at the range of [1.5 s, 4.2 s], [6.3 s, 11s], and [12.9 s, 16.5 s], indicating the end effector is in contact with the environment, the estimated external torques by IEAOB begin to increase, the result demonstrates the effectiveness of the force estimation portion of the algorithm. The non-zero torque estimate arises when the robot is not in contact with the environment and results from running the observers at a relatively large sampling interval. It is easy to see that during contact, the environment rendered force is well tracked by the operator. By contract, Figure 7b shows the force tracking performance of the compared approach A2. In [0.7 s, 3.4 s], [6.4 s, 8.9 s], and [11.7 s, 14.3 s], the estimated external torques start to rise, but it is observed that there is chattering in the estimated torques and the environment

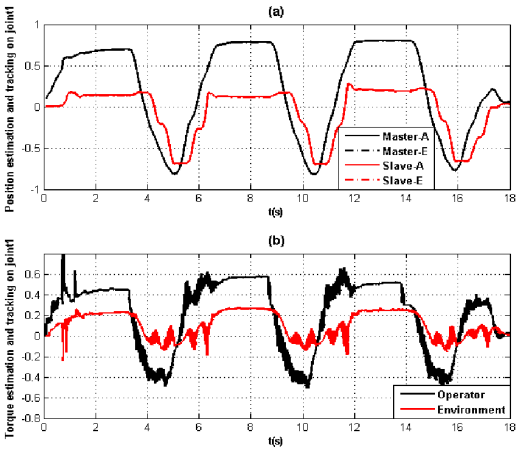

FIGURE 7. Experimental results with the compared teleoperation approach A2 (a) Position response. (b) Force response.

rendered force could not be accurately tracked by the operator because of the inaccurate estimation of the environment force at the slave side. Since 20% parameter variation (M_s, v_{v_s}, v_{c_s} are 20% smaller than the actual values) for the slave robot is assumed in the experiment, the estimated environment force in the approach A2 is smaller than the actual environment forces. Furthermore, Figure 8b demonstrates the force tracking performance of the neural network-based approach A3. Although it shows fair force tracking capability, the number of the neural network weights to be online updated for robot dynamic model identification is very large, which makes it computational demanding. Figures 5 and 6 explain why the proposed approach A1 is superior to the others in terms of position and force tracking. They demonstrate the dynamical parameter and friction estimation performance of the proposed approach A1 for the master robot, slave robot and VIM, respectively, which then are used in the adaptive controller design, it only requires online updating of several dynamic parameters for accurate control design, which is better than the neural network-based approach A3. It is shown that all of the estimation trajectories of robot parameters and friction coefficients in these figures converge to around ($5.0\text{x}10^{-3}$, $-1.5\text{x}10^{-3}$, $1.0\text{x}10^{-3}$), respectively.

C. COMPARISON AND ANALYSIS

The experimental results demonstrate the effectiveness of the proposed robust adaptive observer-based predictive control scheme for nonlinear delayed bilateral teleoperation systems in the presence of system uncertainties and external disturbances. The position and force tracking performance of the Smith predictor-based approach shows the poor ability of the slave manipulator to execute the precise command from the human operator and master manipulator. Since the proposed scheme has the improved ability to cope with the dynamic uncertainties for nonlinear master and slave systems, when there is parameter variation and time delay in the teleoperation system, the proposed teleoperation approach

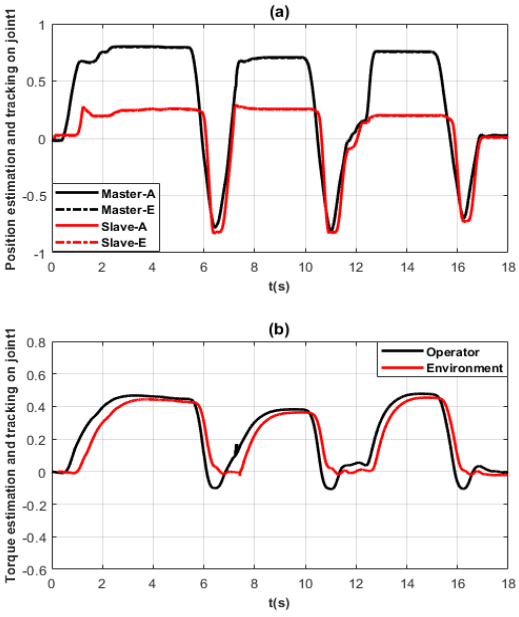

FIGURE 8. Experimental results with the compared teleoperation approach A3 (a) Position response. (b) Force response.

works well in terms of position and force tracking performances, because it can estimate the dynamical parameters and friction coefficients in real time and make them converge to the real values quickly. In comparison with the neural network-based approach, the proposed method reduces less computational cost and offers faster convergence. Since there is no unique guideline to select the topology of neural network and analyze the approximation accuracy, the number of the neural network weights is usually very large, which imposes high computational cost and makes it not competitive in real world applications, and the online estimated weights sometimes suffers from the parameter drifting issue even though theoretical stability is proven.

In summary, the experimental results show that the proposed nonlinear teleoperation design can achieve simultaneous stability and good transparency under time-varying delays, master and slave dynamic uncertainties and external disturbances.

V. CONCLUSION

In this paper, the development and application of a new robust adaptive observer-based predictive control algorithm to achieve teleoperation with high transparency in the presence of communication time-varying delays and nonlinear model uncertainties including robot inertial parameter variations, friction, unmodeled dynamics, and measurement noise was presented. In the proposed method, an adaptive Smith predictor based on the Padé approximation and active observer and sliding mode control is designed to ensure a completed cancellation of the time delay effect. Meanwhile, the IEAOB is deployed at both master and slave sides to obtain accurate robot model estimation as well as external force estimation. Through this control design, some conservative assumptions, such as the upper limit on the time delay changing rate, and the accurate dynamic system model are eased. The stability analysis of the whole system is provided, and finally, experimental evaluation is carried out on a nonlinear teleoperation system built by a pair of Phantom haptic devices. The results demonstrate that the approaches can guarantee simultaneous force and position tracking in bilateral teleoperation systems in the presence of various model uncertainties and time-varying time delay in the communication channels.

REFERENCES

[1] R. H. Taylor and D. Stoianovici, "Medical robotics in computer-integrated surgery," *IEEE Trans. Robot. Automat.*, vol. 19, no. 5, pp. 765–781, Oct. 2003, doi: 10.1109/TRA.2003.817058.

[2] R. Anderson and M. W. Spong, "Bilateral control of teleoperators with time delay," *IEEE Trans. Autom. Control*, vol. 34, no. 5, pp. 494–501, May 1989, doi: 10.1109/9.24201.

[3] J.-H. Ryu, D.-S. Kwon, and B. Hannaford, "Stable teleoperation with time-domain passivity control," *IEEE Trans. Robot. Autom.*, vol. 20, no. 2, pp. 365–373, Apr. 2004, doi: 10.1109/TRA.2004.824689.

[4] G. Niemeyer and J.-J.-E. Slotine, "Stable adaptive teleoperation," *IEEE J. Oceanic Eng.*, vol. 16, no. 1, pp. 152–162, Jan. 1991, doi: 10.1109/48.64895.

[5] G. Niemeyer and J.-J. E. Slotine, "Transient shaping in force-reflecting teleoperation," in *Proc. 5th Int. Conf. Adv. Robot. Robots Unstructured Environ.*, vol. 1, Jun. 1991, pp. 261–266, doi: 10.1109/ICAR.1991.240642.

[6] Y. Ye and P. X. Liu, "Improving trajectory tracking in wave-variable-based teleoperation," *IEEE/ASME Trans. Mechatronics*, vol. 15, no. 2, pp. 321–326, Apr. 2010, doi: 10.1109/TMECH.2009.2020733.

[7] H. Li and K. Kawashima, "Achieving stable tracking in wave-variable-based teleoperation," *IEEE/ASME Trans. Mechatronics*, vol. 19, no. 5, pp. 1574–1582, Oct. 2014, doi: 10.1109/TMECH.2013.2289076.

[8] D. Sun, F. Naghdy, and H. Du, "Wave-variable-based passivity control of four-channel nonlinear bilateral teleoperation system under time delays," *IEEE/ASME Trans. Mechatronics*, vol. 21, no. 1, pp. 238–253, Feb. 2016, doi: 10.1109/TMECH.2015.2442586.

[9] Z. Chen, F. Huang, W. Sun, and W. Song, "An improved wave-variable based four-channel control design in bilateral teleoperation system for time-delay compensation," *IEEE Access*, vol. 6, pp. 12848–12857, 2018, doi: 10.1109/ACCESS.2018.2805782.

[10] A. Denasi, D. Kostic, and H. Nijmeijer, "Time delay compensation in bilateral teleoperations using IMPACT," *IEEE Trans. Control Syst. Technol.*, vol. 21, no. 3, pp. 704–715, May 2013, doi: 10.1109/TCST.2012.2191153.

[11] M. Hamdy, S. Abdelhaleem, and M. Fkirin, "Adaptive fuzzy predictive controller for a class of networked nonlinear systems with time-varying delay," *IEEE Trans. Fuzzy Syst.*, vol. 26, no. 4, pp. 2135–2144, Aug. 2018, doi: 10.1109/TFUZZ.2017.2764851.

[12] K. Natori, T. Tsuji, and K. Ohnishi, "Time delay compensation by communication disturbance observer in bilateral teleoperation systems," in *Proc. 9th IEEE Int. Workshop Adv. Motion Control*, Mar. 2006, pp. 218–223, doi: 10.1109/AMC.2006.1631661.

[13] K. Natori, T. Tsuji, K. Ohnishi, A. Hace, and K. Jezernik, "Time-delay compensation by communication disturbance observer for bilateral teleoperation under time-varying delay," *IEEE Trans. Ind. Electron.*, vol. 57, no. 3, pp. 1050–1062, Mar. 2010, doi: 10.1109/TIE.2009.2028337.

[14] L. Chan, F. Naghdy, and D. Stirling, "Extended active observer for force estimation and disturbance rejection of robotic manipulators," *Robot. Auto. Syst.*, vol. 61, no. 12, pp. 1277–1287, Dec. 2013, doi: 10.1016/j.robot.2013.09.003.

[15] L. Chan, F. Naghdy, and D. Stirling, "Position and force tracking for non-linear haptic telemanipulator under varying delays with an improved extended active observer," *Robot. Auto. Syst.*, vol. 75, pp. 145–160, Jan. 2016, doi: 10.1016/j.robot.2015.10.007.

[16] R. Cortesao, J. Park, and O. Khatib, "Real-time adaptive control for haptic telemanipulation with Kalman active observers," *IEEE Trans. Robot.*, vol. 22, no. 5, pp. 987–999, Oct. 2006, doi: 10.1109/TRO.2006.878787.

[17] Z. Chen, B. Yao, and Q. Wang, "Accurate motion control of linear motors with adaptive robust compensation of nonlinear electromagnetic field effect," *IEEE/ASME Trans. Mechatronics*, vol. 18, no. 3, pp. 1122–1129, Jun. 2013, doi: 10.1109/TMECH.2012.2197217.

[18] W. Sun, H. Pan, and H. Gao, "Filter-based adaptive vibration control for active vehicle suspensions with electrohydraulic actuators," *IEEE Trans. Veh. Technol.*, vol. 65, no. 6, pp. 4619–4626, May 2016, doi: 10.1109/TVT.2015.2437455.

[19] J. Yao and W. Deng, "Active disturbance rejection adaptive control of hydraulic servo systems," *IEEE Trans. Ind. Electron.*, vol. 64, no. 10, pp. 8023–8032, Oct. 2017, doi: 10.1109/TIE.2017.2694382.

[20] J. Yao, W. Deng, and Z. Jiao, "RISE-based adaptive control of hydraulic systems with asymptotic tracking," *IEEE Trans. Autom. Sci. Eng.*, vol. 14, no. 3, pp. 1524–1531, Jul. 2017, doi: 10.1109/TASE.2015.2434393.

[21] M. Sharifi, H. Salarieh, S. Behzadipour, and M. Tavakoli, "Patient-robot-therapist collaboration using resistive impedance controlled tele-robotic systems subjected to time delays," *J. Mech. Robot.*, vol. 10, no. 6, pp. 1–58, Aug. 2018, doi: 10.1115/1.4040961.

[22] H. C. Cho and J. H. Park, "Stable bilateral teleoperation under a time delay using a robust impedance control," *Mechatronics*, vol. 15, no. 5, pp. 611–625, Jun. 2005, doi: 10.1016/j.mechatronics.2004.05.006.

[23] C. Cheng, W. Xu, and J. Shang, "Distributed-torque-based independent joint tracking control of a redundantly actuated parallel robot with two higher kinematic pairs," *IEEE Trans. Ind. Electron.*, vol. 63, no. 2, pp. 1062–1070, Feb. 2016, doi: 10.1109/TIE.2015.2481360.

[24] E. Sariyildiz, R. Oboe, and K. Ohnishi, "Disturbance observer-based robust control and its applications: 35th anniversary overview," *IEEE Trans. Ind. Electron.*, vol. 67, no. 3, pp. 2042–2053, Mar. 2020, doi: 10.1109/TIE.2019.2903752.

[25] Z. Ma, Z. Liu, P. Huang, and Z. Kuang, "Adaptive fractional-order sliding mode control for admittance-based telerobotic system with optimized order and force estimation," *IEEE Trans. Ind. Electron.*, vol. 69, no. 5, pp. 5165–5174, May 2022, doi: 10.1109/TIE.2021.3078385.

[26] D. Sun, F. Naghdy, and H. Du, "Neural network-based passivity control of teleoperation system under time-varying delays," *IEEE Trans. Cybern.*, vol. 47, no. 7, pp. 1666–1680, Jul. 2017, doi: 10.1109/TCYB.2016.2554630.

[27] Z. Chen, F. Huang, W. Sun, J. Gu, and B. Yao, "RBF-neural-network-based adaptive robust control for nonlinear bilateral teleoperation manipulators with uncertainty and time delay," *IEEE/ASME Trans. Mechatronics*, vol. 25, no. 2, pp. 906–918, Apr. 2020, doi: 10.1109/TMECH.2019.2962081.

[28] Z. Chen, F. Huang, W. Chen, J. Zhang, W. Sun, J. Chen, J. Gu, and S. Zhu, "RBFNN-based adaptive sliding mode control design for delayed nonlinear multilateral telerobotic system with cooperative manipulation," *IEEE Trans. Ind. Informat.*, vol. 16, no. 2, pp. 1236–1247, Feb. 2020, doi: 10.1109/TII.2019.2927806.

[29] D. Sun, Q. Liao, T. Stoyanov, A. Kiselev, and A. Loutfi, "Bilateral telerobotic system using type-2 fuzzy neural network based moving horizon estimation force observer for enhancement of environmental force compliance and human perception," *Automatica*, vol. 106, pp. 358–373, Aug. 2019, doi: 10.1016/j.automatica.2019.04.033.

[30] Z. Chen, F. Huang, C. Yang, and B. Yao, "Adaptive fuzzy backstepping control for stable nonlinear bilateral teleoperation manipulators with enhanced transparency performance," *IEEE Trans. Ind. Electron.*, vol. 67, no. 1, pp. 746–756, Jan. 2020, doi: 10.1109/TIE.2019.2898587.

[31] C. Yang, G. Peng, L. Cheng, J. Na, and Z. Li, "Force sensorless admittance control for teleoperation of uncertain robot manipulator using neural networks," *IEEE Trans. Syst., Man, Cybern. Syst.*, vol. 51, no. 5, pp. 3282–3292, May 2021, doi: 10.1109/TSMC.2019.2920870.

[32] L. Chan, "Adaptive observer-based haptic control of nonlinear bilateral teleoperation," Ph.D. Dissertation, School Elect., Comput. Telecommun. Eng., Univ. Wollongong, Wollongong, AU, USA, 2016.

[33] A. Ramasubramanian and L. R. Ray, "Comparison of EKBF-based and classical friction compensation," *J. Dyn. Syst., Meas., Control*, vol. 129, no. 2, pp. 236–242, Jun. 2006, doi: 10.1115/1.2431817.

[34] K. Yoshida and T. Namerikawa, "Predictive PD control for teleoperation with communication time delay," *IFAC Proc. Volumes*, vol. 41, no. 2, pp. 12703–12708, 2008, doi: 10.3182/20080706-5-KR-1001.02149.

[35] A. Probst, O. Sawodny, and M. E. Magaña, "Using a Kalman filter and a Padé approximation to estimate random time delays in a networked feedback control system," *IET Control Theory Appl.*, vol. 4, no. 11, pp. 2263–2272, Nov. 2010, doi: 10.1049/iet-cta.2009.0339.

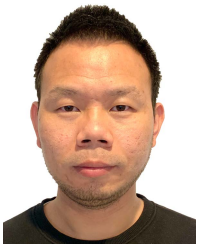

LINPING CHAN received the Ph.D. degree in mechatronics from the School of Electrical, Computer and Telecommunications Engineering, University of Wollongong, Australia, in 2016. He is currently a Research Fellow with the School of Automation, Chongqing University of Posts and Telecommunications. His research interests include robotics, haptic rendering, teleoperation, and intelligent control.

YANG LIU was born in Chengdu, Sichuan, China, in 1998. She received the B.S. degree in automation from the School of Control Engineering, Chengdu University of Information Technology, in 2021. She is currently pursuing the M.S. degree in control engineering with the Chongqing University of Posts and Telecommunications. Her research interests include robotics, teleoperation, industrial Internet of Things, and smart manufacturing.

QINGQING HUANG (Member, IEEE) received the B.S. degree in mechanical engineering and the Ph.D. degree in mechatronic engineering from the College of Mechanical Engineering, Chongqing University, Chongqing, China, in 2009 and 2015, respectively. He is currently an Associate Professor with the College of Automation, Chongqing University of Posts and Telecommunications. From 2017 to 2018, he was a Visiting Fellow with the Faculty of Engineering and Information Sciences, University of Wollongong. His main research interests include robotics, wireless sensor networks, industrial Internet of Things, machine prognostics, and health management.

PING WANG received the B.S. and M.S. degrees from Chongqing University, Chongqing, China, in 1983 and 1988, respectively, and the Ph.D. degree from Southwest Jiaotong University, Chengdu, China, in 1994. He is currently a Full Professor with the College of Automation, Chongqing University of Posts and Telecommunications. His research interests include the intelligent control, industrial Internet of Things, and wireless industrial networks.